

Coalescence and Entrainment: Phenomena on Sieve Trays

A. J. TELLER and R. E. ROOD

University of Florida, Gainesville, Florida

Evaluation was made of the effect of hole spacing for 3/16-in. diameter perforations on a sieve tray, on the magnitude and size distribution of entrainment. The study utilized high-speed photography and entrainment measurements. The magnitude and average particle size of entrainment appears to be related to the degree of bubble coalescence in the liquid continuous phase and increases rapidly with decrease in hole spacing. Bubble bursts do not contribute significantly to entrainment in multiple perforation geometry; the major contribution occurs from shear of the liquid wall by vapor flumes.

Extensive studies have been made with regard to the behavior of the entrainment in sieve trays (1, 2, 3, 8, 9, 11). In general there have been gross correlations of the effect of column velocity, liquid level, surface tension, and tray spacing. Recently a correlation of the quantity of entrainment between the trays as a function of superficial velocity, projection velocity, and particle size distribution (4) was presented.

A significant area of concern that has not been previously investigated is the effect of perforation spacing on the entrainment level in sieve trays. Inasmuch as the hole spacing would have an effect on bubble coalescence, and bubble coalescence results in a release of energy, it was believed that hole spacing would have an effect on the magnitude of entrainment and the size distribution of the projected particles.

Datta et al. (5) indicated the need for such an investigation, and Maier (9), after a preliminary study, indicated that for optimum performance hole spacing should not be less than the average diameter of the bubbles being projected from the perforations.

The formation and development of bubble structure and the relationship to entrainment has also been under investigation in recent years. Newitt (11), utilizing a single perforation, found that entrainment from a single bubble formation was the result of the burst of the bubble at the surface, followed by the rush of liquid into the cavity produced by the burst, and the development of the vertical jet flume. Spells and Bakowski (13, 14) used the high-speed photographic technique to evaluate the bubble formation mechanism in single and multiple bubble cap slots. Two mechanisms were observed: the deep mechanism where

discrete bubbles were formed, and the shallow mechanism where channel bubbling was formed, permitting continual passage of vapor without individual bubble formation. In general the shallow mechanism predominated in multiple slot operation.

Van Krevelen and Hoftijzer (15) found that in the two modes of bubble formation different mechanisms of growth occurred. In the deep mechanism the bubble volume varied with the 1/3 power of the orifice diameter and the bubble volume was independent of flow rate. In the chain bubbling or shallow mechanism the bubble volume increased with flow rate and was independent of the orifice diameter.

It appeared desirable to continue such studies in multiple perforated plates including the effect of interaction of bubbles on the entrainment phenomenon. The high-speed photographic technique was used for observation of the bubble interaction mechanism and the method of Cheng and

Teller (4) for capture and measurement of entrainment.

EQUIPMENT AND PROCEDURE

A Plexiglass column (Figure 1) of rectangular cross section (3×8 in. internal dimensions) was utilized for the study. A segmental inlet seal pan and a segmental outlet weir were utilized to achieve cross-flow behavior. The $3 \times 6 \times \frac{1}{8}$ -in. trays were perforated with three holes, 3/16-in. diameter, on triangular spacings of $\frac{3}{8}$, $\frac{1}{2}$, $\frac{5}{8}$, and $\frac{3}{4}$ in. equivalent in pitch to diameter ratios of 2.00, 2.66, 3.33, and 4.00.

A maximum of three perforations were used to obtain clarity of the high-speed photographs in order to achieve reasonable analysis of the mechanisms of coalescence and entrainment. Inasmuch as the relationship between the quantity of entrainment and height above the tray was analogous to the data obtained by Cheng and Teller (4) for a multiple perforated trap, it is believed that the performance of the three perforation system is reflective of multiple perforation conditions.

Air and water were used as the fluid streams. The air velocity through the perforations was maintained at a constant 53 ft./sec. The liquid flow was maintained

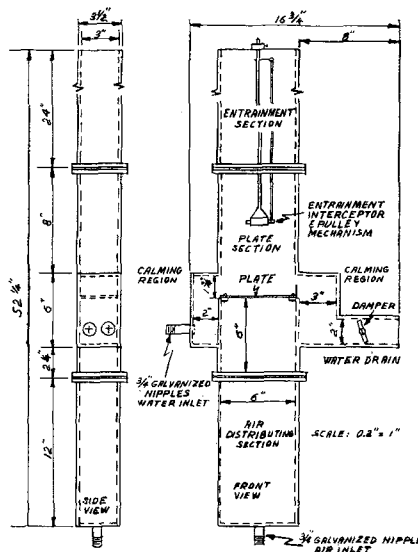


Fig. 1. Detail drawing of column.

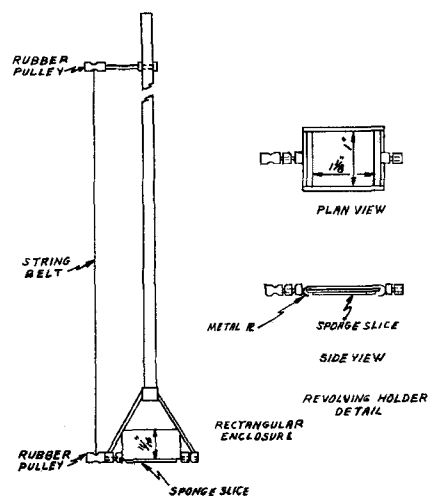


Fig. 2. Entrainment interceptor.

A. J. Teller is with Mass Transfer, Incorporated, Cleveland, Ohio.

constant at a rate of 12 gal./min./ft. of weir. These flows appeared to be a reasonable mean of commercial operating rates. No weeping was observed during the experimental runs.

Entrainment measurements at heights of 4 to 12 in. above the tray were made with the interceptor (Figure 2) suggested by Cheng and Teller (4).

The photographic study was made at a speed of 2,500 frames/sec. with a Fastex WF-14 camera at an $f/4$ opening. Effective lighting was achieved with 3 photo-flood lamps.

BUBBLE FORMATION, COALESCENCE, AND FLUMING

An evaluation of the photographs made for the various perforation spacings indicated in general similar behavior in all four spacings. Variations in this behavior occurred as a result of hole spacing. The general behavior was as follows:

1. Simultaneous or slightly staggered appearance of the three bubbles.

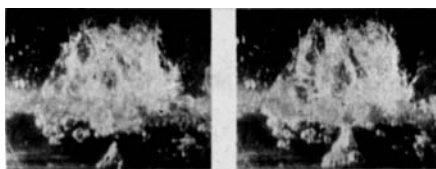


Fig. 3a. Three bubbles formed. b. Bubble growth.

and sheet disintegration. This phenomenon appears evident in the last sequence of Figure 3.

The bubble burst at the liquid surface, a major factor in the entrainment development from single perforations indicated by Newitt (11), does not appear to be significant in the case of multiple perforations. A typical bubble burst is indicated in Figure 4 occurring in 0.0146 sec. The bubble burst appears to consist primarily of a film rollback. The small particles ejected have a significant horizontal velocity vector. As a result of their size (estimated by Newitt to be less than 50μ) and projection direction, they do not appear to contribute significantly to the quantity of entrainment.

COALESCENCE, ENERGY RELEASE, AND MAGNITUDE OF ENTRAINMENT

At the $\frac{3}{8}$ in. spacing the bubbles appeared simultaneously at the three orifices. With increase in perforation

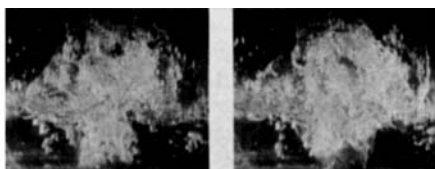


Fig. 3c. Coalescence of bubbles occurring. d. Release of coalesced vapor mass through liquid and flume projection.

Fig. 3. Bubble formation and coalescence.

2. Growth of the bubbles individually (reflecting deep bubbling mechanism).

3. Contact of bubbles.

4. Coalescence of bubbles.

5. Release of the coalesced vapor mass from the plate.

6. Fluming of the mass through the liquid surface causing severe frothing.

7. Filament and sheet disintegration.

An example of this sequence is indicated in Figure 3. The time interval for the entire phenomenon was, in the case shown, 0.0672 sec.

The major mechanism of surface development for the creation of entrainment in the case of multiple perforations appears to be that of filament

spacing there occurred an increasing tendency for staggered appearance of bubbles issuing from the perforations, although simultaneous appearance predominated in all cases. This increasing tendency for nonsimultaneous bubble appearance and the increase of distance between bubbles tended to decrease the degree of coalescence between the bubbles. The Van Krevelen-Hoftizjer relationship indicated that coalescence should occur in all cases, since a bubble diameter of 1.1 in. was possible. However in the $\frac{5}{8}$ and $\frac{3}{4}$ in. spacing coalescence, if it occurred, was achieved primarily in the froth region and not in the liquid continuous zone.

In the phenomenon of coalescence considerable energy is released by the breaking of the liquid film at the juncture of bubbles. The energy release is a function of the surface film destroyed and is equal to $W = \sigma S$. The coalescence of three bubbles results in a decrease in area of about 30% of the initial surface. In the case of the coalescence of three bubbles of $\frac{1}{2}$ -in. diameter the energy release is in the magnitude of 1,300 dyne-cm.

A portion of this energy may be converted into kinetic energy of the vapor and liquid. If the kinetic energy of the gas stream is increased (the volume of gas remaining constant for all cases of hole spacing), such an effect would be observable in the increase in the gas velocity as the gas entered the froth zone. Any increase in velocity would be reflected in a decrease in the diameter of the flume. The flume diameters were therefore measured for the similar conditions of simultaneous three bubble appearance for the four tray spacings.

Sauter mean diameters were obtained for each hole spacing based on a minimum of twenty observations. The results are shown in Table 1.

The decrease in the diameter of the flume in the case of the $\frac{3}{8}$ - and $\frac{1}{2}$ -in. spacings is reflective of a gain in kinetic energy of the gas stream as a result of



Fig. 4a. Bubble burst mechanism. Large bubble formation.

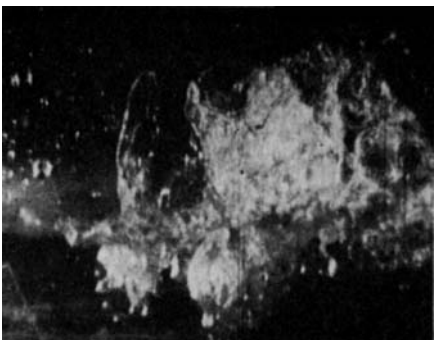


Fig. 4b. Bubble burst mechanism. Film roll back occurring on burst.

TABLE 1. SAUTER MEAN DIAMETERS FOR GAS FLUMES

Hole pitch, in.	$\frac{3}{8}$	$\frac{1}{2}$	$\frac{5}{8}$	$\frac{3}{4}$
Flume diameter in liquid, cm.	3.5	3.5	3.8	4.0
Flume diameter at froth level, cm.	3.2	3.3	3.8	4.0

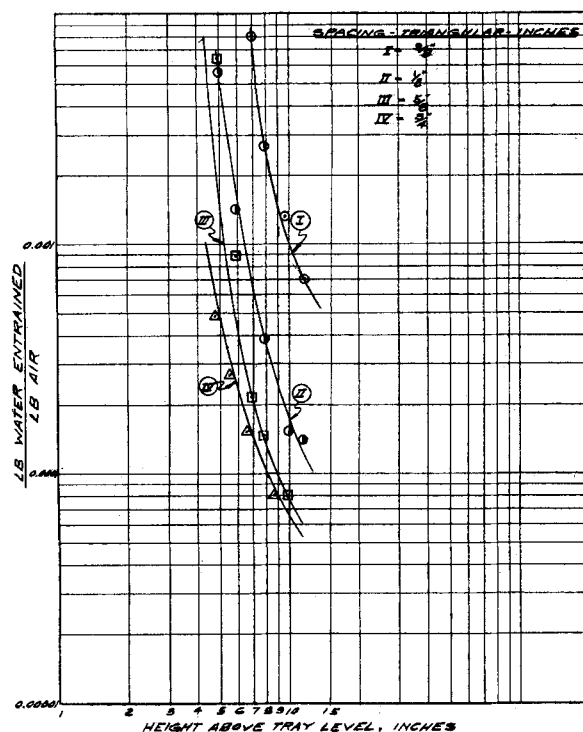


Fig. 5. Entrainment as a function of height above deck.

indicative of the variation in the size of particles projected into the vapor zone as a function of the flume velocity. The relative quantities of entrainment at different levels above the tray for the four hole spacings are shown in Table 2.

The rapid diminution of the ratio of the quantity entrained from the $\frac{3}{8}$ -in. spacing to that at $\frac{3}{4}$ -in. spacing with increase in height above the tray is reflective of the larger particle sizes of liquid projected from the $\frac{3}{8}$ -in. spacing. Inasmuch as the larger particle sizes have higher terminal velocities, their maximum height of ascent is much lower than that of the smaller particles. Thus if the proportion of large particles in a given mass of entrained liquid is large, it would be anticipated that the quantity of entrainment will diminish more rapidly with increased height above the tray than if the particle sizes were smaller.

Entrainment—Particle Size Distribution

An analysis was made to estimate the size distribution of the entrained

particles based on the application of the Davis (6) equation for maximum height of ascent of a particle:

$$H = \frac{q^2}{2g} \left\{ \ln \left[1 + \left(\frac{P-u}{q} \right)^2 \right] \right\}$$

$$- \ln \left[1 - \left(\frac{u}{q} \right)^2 \right] \right\} + \frac{uq}{2g} \left[2 \tan^{-1} \left(\frac{p-u}{q} \right) + \ln \left(\frac{q+u}{u} \right) \right]$$

Projection velocities were obtained from the data of Akselrod and Yusova (3) and terminal settling velocities from that of Perry (12). The superficial column velocity was 0.24 ft./sec. The size distribution was obtained from the maximum height attained by the different particle sizes (Figure 6) and the decrease in weight of the entrained liquid as a function of height above the clear liquid.

The particle size distribution based on this analysis is indicated in Figure 7. Inasmuch as measurements were made at levels in proximity to the froth, these particles dropping out at levels up to 8 in. above the froth were 600 μ and greater. Via summation of the quantity of these particles a distribution of particle sizes ranging from 600 to 8,000 μ was obtained at a level of 2 in. above the froth. The distribution indicated in Figure 7 is logarithmic in nature and confirms the existence of this type of distribution for particle sizes ranging between 200 and 2,000 μ as obtained by Chang and Teller (4) for multiple perforated trays.

Note that a major portion of the energy released for liquid entrainment is utilized for the projection of the

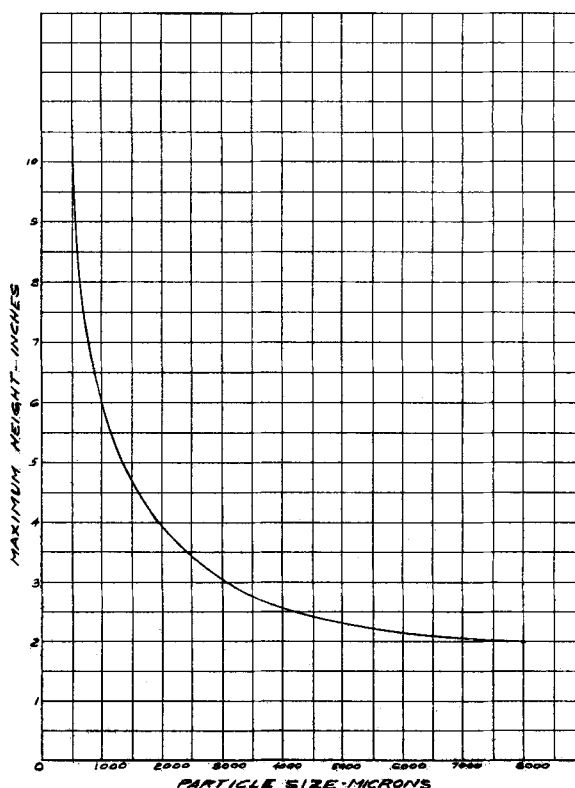


Fig. 6. Maximum height achieved as function of particle size.

TABLE 2. RELATIVE ENTRAINMENT AT SPECIFIC HOLE SPACING

Height above tray, in.	3/8	Hole spacing Inches		
		1/2	5/8	3/4
7	59	4.7	1.46	1
8	23	3.5	1.27	1
10	15	2.5	1.14	1
12	13.6	2.2	1.10	1

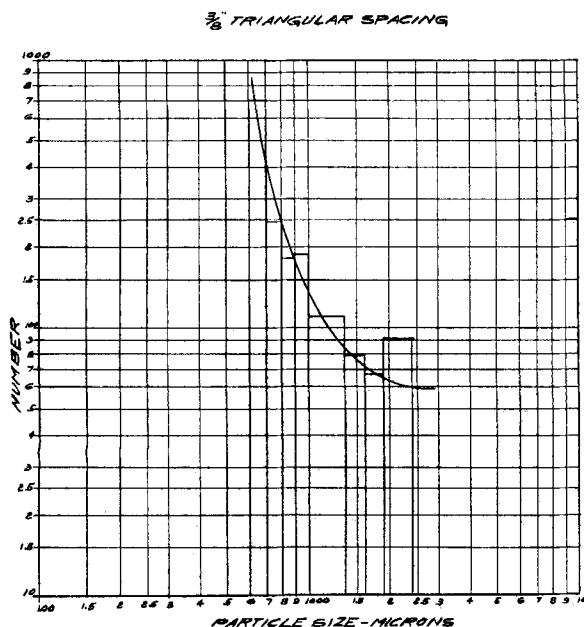


Fig. 7a. Particle size distribution in entrained liquid.

larger size particles, and with increase in energy transfer (as occurring at the $\frac{3}{8}$ - and $\frac{1}{2}$ -in. spacings) an increasing proportion of the energy released is converted into projection of particles greater than $2,000 \mu$ in size.

The lack of contraction of the flume in the cases of the $\frac{5}{8}$ - and $\frac{3}{4}$ -in. spacings (Table 2) appears to agree well with the similar energy transferred to the development of particle surface in

these cases. Where contraction occurs, a rapid increase in energy release also occurs.

A quantitative relationship between the degree of coalescence is not obtainable. Much of the energy utilized in the formation of entrained particles is consumed in viscous losses. Total coalescence based on 5,700 cycles/lb. of air for bubble release would result in an energy transfer of the magnitude of

3×10^6 erg./lb of air flow. This is several magnitudes greater than that estimated for particle surface development. However the variation of flume diameter indicates that the air flow through the flume in the froth area has significantly greater energy content in the cases of the $\frac{3}{8}$ -in. spacing (2×10^6 erg./lb. of air) and the $\frac{1}{2}$ -in. spacing (1×10^6 erg./lb. of air) than the larger hole spacings. These changes in energy content imply that in the case of the $\frac{3}{8}$ -in. spacing approximately two-thirds of the bubble coalescence occurs in the liquid continuous phase; approximately one-third of the coalescence phenomena occur in the liquid continuous phase in the $\frac{1}{2}$ -in. spacing and little or none in the $\frac{5}{8}$ - and $\frac{3}{4}$ -in. spacings.

NOTATION

- H = height of ascent of particle, ft.
 g = acceleration of gravity, 32 ft./
(sec.)²
 P = projection velocity of particle,
ft./sec.
 q = terminal velocity of particle,
ft./sec.
 S = surface of bubble, sq.cm.
 u = superficial vapor velocity, ft./
sec.
 w = energy, erg.
 σ = surface tension, dynes/cm.

LITERATURE CITED

1. American Institute of Chemical Engineers, "A.I.Ch.E. Bubble Cap Manual," A.I.Ch.E. Research Committee, New York (1958).
2. Atteridge, P. T., F. J. Lemieux, W. C. Schreiner, and R. A. Sundback, *A.I.Ch.E. Journal*, **2**, 3 (1956).
3. Axelrod, L. S., and J. Yosuva, *J. App. Chem. USSR*, **30**, 739 (1957).
4. Cheng, S. I., and A. J. Teller, *A.I.Ch.E. Journal*, **7**, 282 (1961).
5. Datta, R. L., D. H. Napier, and D. M. Newitt, *Trans. Inst. Chem. Engrs.*, **28**, 14 (1950).
6. Davis, R. F., *Proc. Inst. Mech. Engrs.*, **144**, 216 (1940).
7. Eduljee, H. E., *Brit. Chem. Eng.*, **4**, No. 6, p. 320 (1959).
8. Hunt, C. d'A., D. N. Hanson, and C. R. Wilke, *A.I.Ch.E. Journal*, **1**, No. 4, p. 441 (1955).
9. Maier, C. Ct., *U.S. Bur. Mines Bull.*, **260**, 62 (1927).
10. Muller, H. M., and D. F. Othmer, *Ind. Eng. Chem.*, **51**, 625 (1959).
11. Newitt, D. M., N. Dombrowski, and F. H. Knelman, *Trans. Inst. Chem. Engrs.*, **32**, 244 (1954).
12. Perry, J. M., "Chemical Engineers' Handbook," McGraw Hill, New York.
13. Spells, K. E., and S. Bakowski, *Trans. Inst. Chem. Engrs.*, **28**, 33 (1950).
14. *Ibid.*, **30**, 189 (1952).
15. Van Krevelen, D. W., and P. J. Hoftijzer, *Chem. Eng. Progr.*, **46**, 29 (1950).

Manuscript received May 2, 1961; revision received November 22, 1961; paper accepted November 22, 1961. Paper presented at A.I.Ch.E. Cleveland meeting.

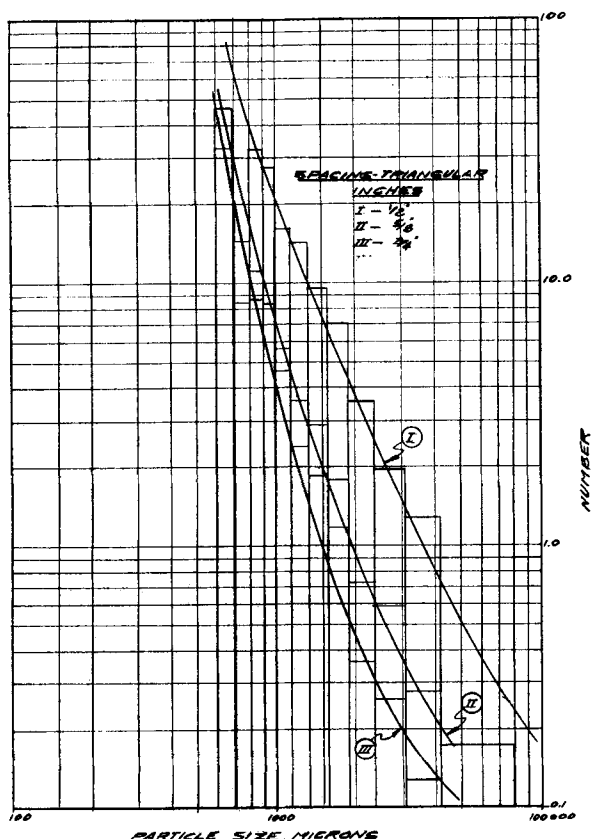


Fig. 7b. Particle size distribution in entrained liquid.